

01 Jan 2023

Analyzing The Effectiveness Of The Gurney Method For Small Scale Fragmentation Propulsion Using Exploding Bridgewire Detonators

Emily M. Johnson

Rachel L. Bauer

Catherine E. Johnson

Missouri University of Science and Technology, johnsonce@mst.edu

Follow this and additional works at: https://scholarsmine.mst.edu/min_nuceng_facwork

 Part of the [Explosives Engineering Commons](#)

Recommended Citation

E. M. Johnson et al., "Analyzing The Effectiveness Of The Gurney Method For Small Scale Fragmentation Propulsion Using Exploding Bridgewire Detonators," *Propellants, Explosives, Pyrotechnics*, Wiley, Jan 2023.

The definitive version is available at <https://doi.org/10.1002/prop.202200246>

This Article - Journal is brought to you for free and open access by Scholars' Mine. It has been accepted for inclusion in Mining Engineering Faculty Research & Creative Works by an authorized administrator of Scholars' Mine. This work is protected by U. S. Copyright Law. Unauthorized use including reproduction for redistribution requires the permission of the copyright holder. For more information, please contact scholarsmine@mst.edu.

RESEARCH ARTICLE

Analyzing the effectiveness of the Gurney method for small scale fragmentation propulsion using Exploding Bridgewire detonators

Emily M. Johnson²  | Rachel L. Bauer² | Catherine E. Johnson¹

¹Mining and Explosives Engineering, Missouri University of Science and Technology, 290 McNutt Hall, Rolla MO

²Mining and Explosives Engineering, Missouri University of Science and Technology, Rolla MO

Correspondence

Catherine E. Johnson, Mining and Explosives Engineering, Missouri University of Science and Technology, 290 McNutt Hall, 1400 Bishop Ave., 65409, Rolla MO.

Email: Catherine.johnson@mst.edu

Funding information

Missouri University of Science and Technology Energetics Research Team

Abstract

Explosives are common in military, mining, and construction applications where the explosive properties are understood, but mechanics of how the explosive's energy fragments and throws materials are less known. Considering the type of confining material around an explosive, creates variability in fragmentation behavior due to the individual material characteristics. The most common method for assessing fragmentation behavior is the Gurney method, which eliminates any consideration of fragmenting material properties. The Gurney method assumes that, on a large scale, the inconsistencies in material are irrelevant and only the mass of the confiner need be considered. However, it is known in many fields that energy is consumed in the breaking of a material. In this paper, the detonation and resultant fragmentation propulsion of Exploding Bridgewire (EBW) detonators with the same explosive material, but different casing characteristics, is observed. The Gurney method was used to predict fragmentation velocities of the casing following detonation, which were compared to the behavior observed through high-speed video of the actual event. The EBWs were selected to provide variability in casing material, casing thickness, charge length, and charge diameter. It was found that when the amount of explosive is small, the material properties of the casing play a significant role, with 70% of the total explosive mass lost in fragmenting PMMA EBWs and $30 \pm 3\%$ lost in Aluminum EBWs. There is significant energy loss to breaking the casing material that cannot be ignored on the small scale and could impact large explosives with high casing to explosive ratios.

KEYWORDS

energy distribution, exploding bridgewire detonator, explosive, gurney model, projectile frag

1 | INTRODUCTION

One of the most common shapes for an explosive used in both industry and military applications, is the cylinder [1–3]. Cylindrically shaped explosive charges are also one of the most well understood and documented types of charges [1–5]. The blast wave expansion from a

cylindrical charge has been studied extensively, resulting in the development of experimentally derived equations that can predict the peak pressure of a blast wave at any distance and in any direction after detonation [1–5]. Figure 1 shows the widely accepted and observed bell-shaped blast wave that results from the detonation of a bare cylindrical charge, where the arrow out the flat end

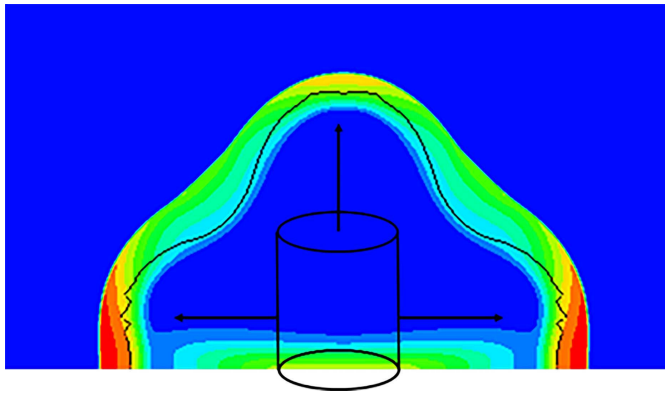


FIGURE 1 Blast wave form of bare cylindrical charge.

of the charge denotes the axial direction and the arrow out the curved side denotes the radial direction. The addition of casing material in the radial and/or axial direction will change the rate of expansion in each direction and introduce fragmentation (frag) into the energy distribution and expansion factors [6–8].

Due to the high variability in the resultant blast and frag behavior that results from changes in casing mass, density, and thickness; there is less consensus on how a cased cylindrical charge will behave [6, 8–11]. There is, however, a common method, known as the Gurney method, for estimating the behavior of the fragmented casing post blast [6, 11–15]. The Gurney method estimates the division of energy released during detonation between the blast wave and the casing fragmentation for various geometries [16–18]. It was originally created for the calculation of velocity of the projectile frag resulting from large military explosives, such as grenades or improvised explosive devices (IEDs) [16, 17]. The method involves making four basic assumptions: (1) energy and momentum are conserved before and after detonation; (2) all of the potential chemical energy is transferred to mechanical energy of either the projectile frag or the blast wave; (3) the density of gas products before the casing begins moving is uniform; and (4) the velocity of the product gas increases linearly from zero at the center of mass to terminal velocity of the casing at the interface between the casing and the product gas [17]. The last two assumptions are key in representing the amount of energy allocated to the blast wave. All four assumptions allow for the derivation of a model representing the fragmentation velocity of a cased charge, Figure 2.

Figure 2 depicts a cylindrical explosive charge, cased on its curved side, the sides, and on one flat end, the end. The casing has been split into two distinct pieces, end and side, to differentiate the propelled frag by direction of travel and maximum velocity. This means

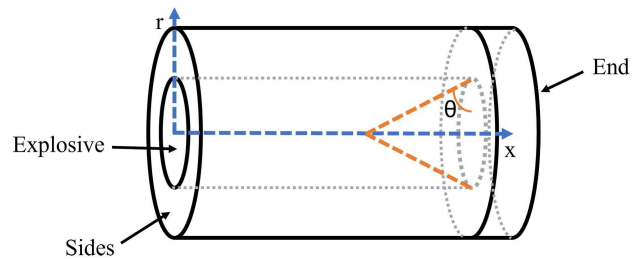


FIGURE 2 Cylindrical charge cased around sides and end: orange outlines the cone of effective explosive mass and blue shows the axis of direction x is axial, r is radial.

separate equations are used to calculate the fragmentation velocity of each section of casing material.

The equation used to estimate the velocity of the sides of the casing is Equation 1 [15–18], where E is the specific chemical energy of the explosive, ϕ is the mass of the sides, and C_s is the mass of explosive acting on the sides. It is assumed that all the chemical energy produced by C_s is acting in the radial direction.

$$V_{\text{side}} = \sqrt{\frac{2E}{\frac{\phi}{C_s} + \frac{1}{2}}} \quad (1)$$

The velocity of the end frag is estimated from what is known as the “open-faced sandwich” equation, shown in Equation 2 [15–18]. Here E is the specific chemical energy, C_a is the mass of explosive acting on the end, and M is the mass of the end disk, where the end disk is defined as the casing that rests on the flat end of the explosive cylinder.

$$V_{\text{end}} = \sqrt{2E \left[\frac{1 + \left(1 + \frac{2M}{C_a}\right)^3}{6 \left(1 + \frac{M}{C_a}\right)} + \frac{M}{C_a} \right]^{-1/2}} \quad (2)$$

The distribution of the total explosive mass allocated to moving either the end or sides is determined by the ratio of casing mass around the sides, ϕ , of the charge and the mass of explosive held within it, C . In Equation 3 [15–18], this ratio is used to define the base angle of the cone in Figure 2 with a base diameter equal to the inner diameter of the casing, that’s fully coupled with the explosive. This cone represents a volume of explosive with a mass equivalent to the mass acting on the end, C_a . The remaining explosive mass, C_s , is equivalent to the mass acting on the sides.

$$\theta = 90 - \frac{30}{\sqrt{\frac{2\phi}{C} + 1}} \quad (3)$$

TABLE 1 Detonator Casing and Explosive Characteristics.

EBW (-)	Diameter (cm)	Casing thickness (cm)	Length (cm)	Casing mat (-)	Casing ρ (g cm ⁻³)	Mass PETN (mg)	Mass HMX w/Binder (mg)
RP-501	0.75	0.018	0.309	Al	2.785	169	227
RP-502	0.75	0.018	0.613	Al	2.785	136	450
RP-503	0.98	0.079	0.467	PMMA	1.18	167	454
RP-83	0.71	0.018	1.380	Al	2.785	209	908

Figure 2 shows a cone that fits well within the explosive cylinder as its height is far shorter than the length of the charge. However, if the base angle of that cone were to increase, due to an increase in the mass of the sides, or if the length of the explosive cylinder were to decrease, the height of the cone could exceed the length of the explosive cylinder. This would mean the tip of the cone outside the cylinder would not be included in the explosive mass acting on the end. Consider the charge in Figure 2, if the length of the charge and casing is decreased to 3/4ths its original length from the uncased end, the size of the cone is unaffected. This means that only the explosive mass acting on the sides is affected by shortening the charge length until the length of the charge is shorter than the height of the cone.

As Equations 1–3 were developed to represent large explosive devices, such as grenades or pipe bombs, assumption number two, that all potential chemical energy is converted to mechanical energy, has been easily accepted as truth. For large charges, the energy needed to break the casing around the explosive into frag is negligible compared to the energy produced by a large quantity of explosive [17, 18]. Recent studies into how the Gurney method can be adapted to predict the blast wave behavior of cased charges have given rise to the question of whether this assumption applies to small explosives, such as detonators [6, 7, 19, 20]. One study showed that the Gurney method was only accurate in the prediction of blast wave expansion to within 13% for an electronic detonator [19]. Questions arise as to how accurate the Gurney method is at representing frag when the system is scaled down to the point that the explosive energy produced no longer far exceeds the energy required to break the casing and at what charge to casing mass ratio this occurs.

This paper investigates the detonation and resultant frag propulsion of Exploding Bridgewire (EBW) detonators with the same explosive material, but different casing characteristics. The Gurney method is used to predict frag velocities, the predictions are compared to experimental results observed through high-speed video.

2 | EXPERIMENTAL SECTION

2.1 | Experimental method

A series of experiments were conducted to capture the frag velocities in the axial and radial directions from EBWs. An EBW is a type of detonator that uses an exploding bridge wire to initiate the column of explosive housed in its casing. This bridgewire releases minimal to no gases when it explodes and initiates the explosive via shock initiation. Alternatively, other detonator types use hot wire or pyrotechnic delay to initiate the explosive column. These devices release additional product gas and chemical energy which contribute to the detonator performance. This made the EBW the optimal choice for this test series. The EBW design not only allows for timing precision in primary column initiation, but also limits the energy sources that contribute to the casing expansion.

Each EBW was fed through a hole at the center of a 0.61 m × 0.61 m × 0.635 cm steel table so that the column of explosive in each, listed in Table 1, was well above the surface of the table. The table was positioned 9 m from the test bunker at the Missouri S&T Experimental Mine. A Phantom high-speed camera [21] was used to film the frag and shock propagation across the tabletop from the safety of the concrete bunker. Each detonator was filmed at a rate of 100,000 frames per second. The phantom was triggered using a thin copper trigger wire across the top, or flat end, of the detonator. The test configuration can be seen in Figure 3. Each EBW was tested three times to verify consistency of behavior.

Four different EBWs were chosen for this study: (1) RP-83, (2) RP-501, (3) RP-502, and (4) RP-503 [22]. Each detonator was chosen to compare different casing characteristics. A description of the dimensions and casing material for each detonator and their explosive contents is listed in Table 1 [15, 22–24]. The detonators all contain PETN at a density of 0.9 g cm⁻³ and HMX with binder at a density of 1.8 g cm⁻³. The Gurney energy ($\sqrt{2E}$) of the explosive contents are 1.85 and 2.89 km s⁻¹ respectively

[24–28]. The casing material for each detonator is either aluminum metal (Al) or Polymethyl methacrylate (PMMA). The dimensions of the detonators are the measured diameter and the length that protrudes out the surface of the tabletop test plate. The diameter was measured from each EBW and the casing thickness was provided by the manufacturer's product data sheets. The length was estimated from the diameter, casing thickness, and theoretical maximum density of the explosive. The tests for each EBW were repeated three times to account for outliers.

2.2 | Methodology of Gurney calculations

Table 2 gives the calculated Gurney parameters for each EBW. Table 3 shows the predicted velocity for frag from the end and sides of each EBW. M and ψ were calculated as a product of density and volume. For the purposes of this study the volume of the end is defined by a cylinder with a diameter equal to the outer diameter of the detonator and a length equal to the thickness of the casing. The volume of the sides is that of a hollow cylinder. θ was found from Equation 3 and h_a is the height of the cone. From here the volume, V_a , and equivalent mass to the end, C_a , was calculated. Lastly the velocities of the end and sides were found from Equations 1 and 2.

This method predicts that the end velocity will be consistently higher than the sides. It also predicts that the end velocities will increase as follows: $503 < 501 <$

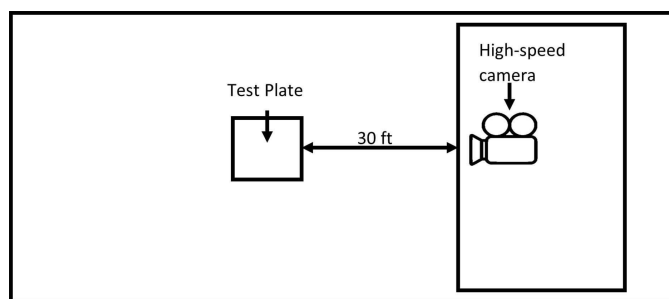


FIGURE 3 Position of camera with respect to the test plate.

TABLE 2 Predicting the end and side velocity of each detonator parameters.

EBW (-)	M (g)	Ψ (g)	Θ (rad)	h_a (cm)	V_a (cm^3)
RP-501	0.02	0.08	1.13	0.76	0.10
RP-502	0.02	0.11	1.12	0.75	0.10
RP-503	0.07	0.21	1.16	0.96	0.17
RP-83	0.02	0.22	1.13	0.71	0.08

$502 < 83$. This order appears to result from the relationship between the end frag mass and the contributing explosive mass. Similarly, the side velocities increase as follows: $503 < 501 < 502 < 83$. The end velocity for the 502 is slightly higher than that of the 83 (by about 40 m/s) due to the slightly smaller diameter of the 83.

3 | RESULTS AND DISCUSSION

In this section the high-speed videos are analyzed and the direction of flight of the propelled frag is discussed. The velocities of the frag in each direction are then compared to respective predicted velocities calculated using the Gurney method. Also, the effect of detonator design properties will be evaluated by relating design parameters to the frag velocity.

High-speed video was used to observe each detonator, as seen in Figure 4. This figure shows the energy expanding in 2 directions, axially up (0 degrees) and radially to the sides (90 degrees). Figure 4b and 4c show a very clear energy expansion of the end and sides of the detonator. There is no gas product expansion in the direction between 30 degrees and 60 degrees. The gas expansion in the radial and axial directions shown as black arrows in Figure 4b is moving too fast for the gas shock wave to be seen in those directions. The gas shock can be seen, however, in the gap between the two directional fronts as outlined in Figure 4c. As the shock expands, it moves as two separate waves. The first is a cone out the end expanding in tip angle and height as the wave slowly catches up to the end frag seen in Figure 4d. The

TABLE 3 Effective mass and predicted velocities.

EBW (-)	C_a (g)	V_{end} (km s^{-1})	C_s (g)	V_{side} (km s^{-1})
RP-501	0.14	2.87	0.26	2.53
RP-502	0.15	3.25	0.44	2.90
RP-503	0.25	2.70	0.37	2.41
RP-83	0.13	3.34	0.99	3.04

second is a hemisphere expanding from the radial energy release. There is a line denoting a high-pressure region where the two waves collide. These observations indicate that the detonator behaves as two separate energy releases that do not interact until expansion occurs.

Each high-speed video was analyzed and the velocity of the leading piece of frag was measured out the end and each side of the detonator in the first 100 μ s after detonation. The velocities were calculated as a relationship between distance and time in each frame. Three repetitions allowed an average and variance to be calculated for each EBW. The predicted end and side velocities calculated in Table 3 (PV_{end} , PV_{side}) are compared to these measured end and side velocities (MV_{end} , MV_{side}) in Table 4. The spread of velocities from each EBW type can be seen in Figure 5 through Figure 8.

In Table 4, the predicted velocities are much higher in both directions than those observed through experimentation. The Gurney prediction method assumes that the casing around the sides and end of the explosive are two separate pieces. This means, in the predictive model, there is no energy consumed during the separation of these two pieces. In reality, the detonators RP-501, RP-502, and RP-83 are manufactured through

drawn metal stamping, meaning the casing is one piece of metal. This means that the energy required to separate the end from the sides is the same as that required to fragment either piece into smaller pieces. The casing around the sides and on the end of RP-503, on the other hand, are glued together, creating additional resistance to separation and a hard right angle between the sides and end of the casing, unlike the stamped detonators. The percentage difference in kinetic energy of the frag between the predicted velocities and measured are listed in Table 5. The total difference was calculated from the sum of the end and side kinetic energies and compared to the total potential chemical energy of the explosive in each EBW.

From Table 5 it can be seen that the EBW with the lowest energy difference is the RP-503. This could be a result of the strength of the PMMA casing compared to the aluminum. Aluminum is known to have a higher tensile strength than PMMA, meaning more energy would be consumed in breaking it. However, the PMMA casing is also over four times thicker than the aluminum and the inner diameter of the PMMA casing is larger. Both of these variables could result in an increased amount of energy required to break the PMMA casing compared to the Aluminum. An alternate explanation for the decreased energy loss the casing manufacture method used for the detonator. Breaking the glued casing would likely consume less energy than breaking the

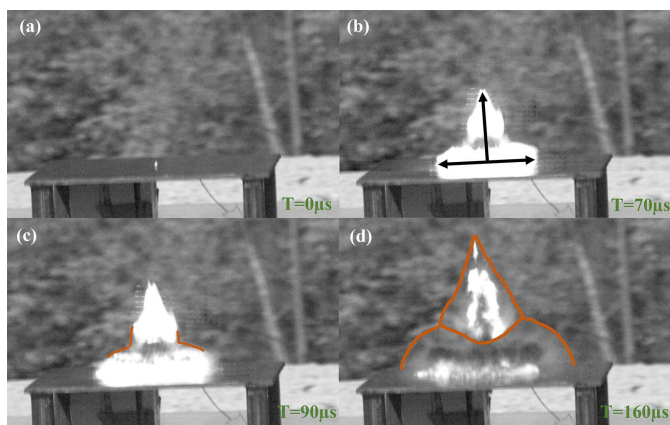


FIGURE 4 503 video observation, (a) uninitiated cap at time = 0; (b) observed radial and axial expansion from detonator at time = 70 μ s; (c) outline of shock in air between two expanding directions at time = 90 μ s, (d) shock expansion beyond fireball continues at time = 160 μ s.

TABLE 4 Predicted (PV) and measured (MV) frag velocities.

EBW (-)	PV_{end} (km s^{-1})	MV_{end} (km s^{-1})	PV_{side} (km s^{-1})	MV_{side} (km s^{-1})
RP-501	2.87	2.36 ± 0.061	2.53	1.65 ± 0.083
RP-502	3.25	3.12 ± 0.063	2.90	1.93 ± 0.056
RP-503	2.70	2.69 ± 0.076	2.41	1.95 ± 0.061
RP-83	3.34	3.26 ± 0.055	3.04	2.38 ± 0.091

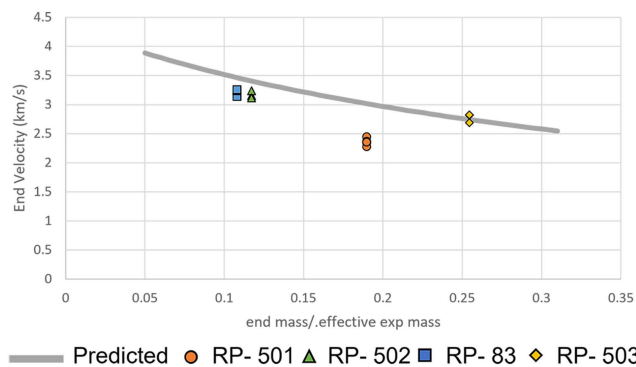


FIGURE 5 Relationship between the velocity of the end and the ratio of end mass to explosive mass acting on the end.

TABLE 5 Percent difference in kinetic energy of frag between the predicted and measured velocities.

EBW	%END	%SIDES	%TOTAL
RP-501	49	133	81
RP-502	8	126	48
RP-503	1	52	21
RP-83	5	64	28

stamped casing due to both the angle of the end to the sides of the detonator and the glue providing less resistance than the metal of the drawn metal stamped detonators. Despite the decreased resistance, the energy loss to the sides is significantly higher than out the end. Looking at the aluminum cased detonators, the energy loss disparity decreases as the mass of explosive, or the length of the detonator, increases. The energy loss to the end is consistently lower than that to the sides. This indicates that a larger percentage of the explosive energy causes the end frag. It could also suggest that the velocity equation for the end is more accurate. However, given the total energy loss observed is very close to the average observed in both direction, the accuracy of both equations appear to be comparable. From both Table 4 and Table 5 one can conclude that the Gurney model becomes more accurate as the tensile strength of the casing decreases or as the explosive mass increases. This demonstrates that energy consumed in breaking the casing material is not negligible compared to the energy produced by the explosive. This theory is further supported by the comparison of the observed velocities and the theoretical velocities of frag with increasing casing mass to explosive mass ratios, shown in Figure 5 and Figure 6. To compare the performance of the detonators based on mass of explosive, an equivalent mass of TNT was found using equations 1 and 2. With an equivalent mass of TNT, the explosive is standardized between each detonator and can be easily compared. These equivalent masses, found in Table 6, are used to standardize the explosive type in Figures 5 through Figure 8 and Table 7.

In Figures 5 and Figure 6 two things are seen: (1) the 503 is closer to theoretical than the other three, likely due to casing method, and (2) despite the other 3

TABLE 6 Detonator Initiating Explosive Parameters.

EBW (-)	Top mass TNT (g)	Side mass TNT (g)	TOT TNT (g)
RP-501	0.12	0.21	0.32
RP-502	0.19	0.60	0.79
RP-503	0.31	0.42	0.727
RP-83	0.19	1.78	1.97

TABLE 7 Mass Lost; mass used is the mass of explosive needed to produce observed frag velocities and the percent of mass unused is the percent of the total explosive mass that is not contributing to produce the observed frag velocities.

EBW (-)	End mass used (g)	TNT end mass unused (%)	Side mass used (g)	TNT side mass unused (%)
RP-501	0.066	43	0.052	75
RP-502	0.156	16	0.106	82
RP-83	0.172	11	0.415	77
RP-503	0.303	1	0.205	51

detonators theoretically having end velocities that fall within 0.13 km s^{-1} of each other, only the larger mass/longer length detonators, the RP-502 and RP-83, have velocities which follow this trend.

A closer look at the RP-503 shows the end velocity is more accurate compared to the predicted velocity than that of the sides. The side velocities are more precise in their distance from the predicted line in Figure 6. The variance observed in the end velocities indicates that the amount of energy consumed to break the glued casing may have been inconsistent between detonators, but regardless the same amount of energy went to breaking and throwing the side casing with each test. Considering the energy distribution between the ends and sides discussed in Equation 1, it appears that the mass of explosive acting in either the axial or radial direction has a constant distribution between repetitions. Only the end energy appears to be affected by the inconstancy in energy consumed to break the glue.

Given the near equivalent end mass to effective explosive mass of the RP-501, RP-502, and RP-83, one should see near constant end velocities between these three EBWs. Looking at the predicted end velocities for these detonators, the largest difference in end velocity among them is no more than 150 m/s. The observed velocities for the RP-502 and RP-83 match this prediction with a difference in velocity of 140 m/s. However, the velocity for the RP-501 is nearly 1,000 m/s lower than the others. RP-501 has the lowest total mass of HMX,

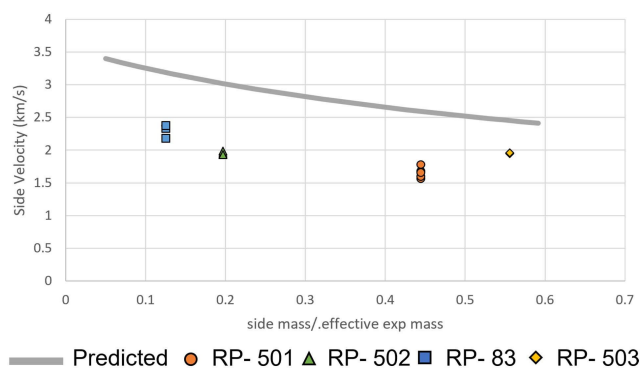


FIGURE 6 Relationship between the velocity of the side frag and the ratio of side mass to explosive mass acting on the sides.

meaning the shortest length. This might affect the effective mass of explosive available to act out the end of the detonator.

Figure 6 shows that the side mass to effective mass ratio for the three aluminum cased detonators are not the same. The slope of their velocities is much steeper than the predicted. The rate at which the velocities increase with decreasing mass ratio is also higher than the predicted. This hints at two things: (1) the equation used to find the effective mass of explosive is ineffective for these EBWs and (2) the tensile strength of the material plays a role. For the first note, the cone of explosive acting on the end (Figure 2) may extend farther than the length available. This is shown by the change in slope between the points. As the length increases, the velocity of the sides increases. On the second note, the tensile strength of the material is relative to the force acting over a set area.

Stamped detonators show more energy loss to fragmentation than glued detonators. The source of this energy loss cannot be evaluated using Gurney equations as they do not consider breaking the casing. Material properties such as tensile strength will affect the energy loss.

In Figure 7 and Figure 8, the three aluminum detonators, which were all stamped, are compared to the predicted model. From these curves a correlation between the stamped energy loss, tensile stress, and explosive energy consumed can be drawn. Figure 7 compares the total mass of explosive with the velocities of the end frag both observed and predicted. Similar to Figure 6, this graph shows that the energy loss from breaking is not the only source of velocity increase. Given the constant casing thickness of these detonators, if the breaking energy loss were the only factor, the velocities of the three EBWs would form a near straight line, as the amount of energy consumed for each to break would be constant. Instead, it appears that the breaking has affected distribution of explosive mass applied to either the end or the sides.

The curve seen for the theoretical side velocity in Figure 8, follows a logarithmic increase. The real observed data follows a linear increase. These patterns contradict each other as while Gurney says that limit to the side frag velocity is 3.4 km s^{-1} the experimental suggests that no such limit exists. The unaligned pattern observed is different from Figure 7 as while the two data sets were separated by magnitude, they followed that same pattern of increase. This suggests that these three detonators are representative of a much smaller segment of the theoretical graph than is indicated here. It looks linear because it is “zoomed in”.

To test this theory, Equation 3 was adapted to align the theoretical and projected data sets. Looking at the

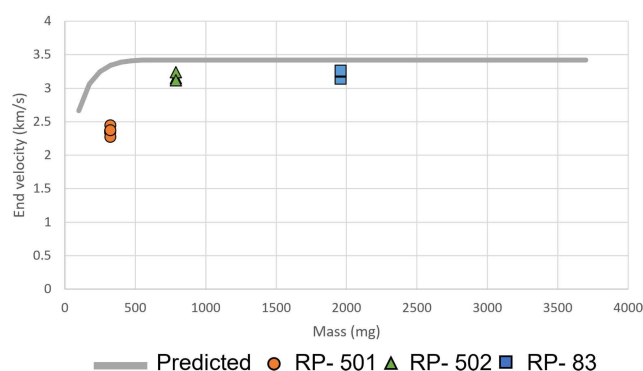


FIGURE 7 Aluminum EBWs End; relationship between the velocity of the end and the total mass of explosive.

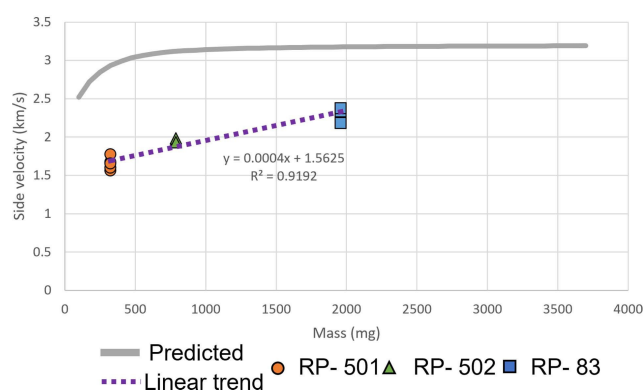


FIGURE 8 Aluminum EBWs Side; relationship between the velocity of the sides and the total mass of explosive.

mass of explosive that would propel the frag out the end and the sides at the speeds observed gave an idea of how much of the explosive mass went toward breaking the casing. Table 7 lists the mass that was needed to propel the frag in either direction at the observed velocities, the residual mass that was not used in either direction, and the percent of the total explosive mass in either direction the residual accounts for. The mass needed was calculated by rearranging the gurney equations and plugging in the experimentally observed frag velocity. The residual mass is the difference between the mass contained within each detonator and the mass needed.

From Table 7 it is seen that for the aluminum EBWs, percent of mass that goes to breaking the sides remains constant with a standard deviation between percent TNT mass of 4%. This indicates that a set mass went toward reaching a constant tensile stress along the wall. The percent of the end mass used to break it decreased with increasing total explosive mass. This might result from the sides fragmenting faster at higher masses, reducing the need for the end to break, before it flies. There is no correlation between the aluminum and the PMMA EBWs and the tensile strength of the PMMA is different

from the Aluminum. It can be noted that the needed mass percentage to break the sides of the PMMA EBW was lower than the aluminum ones. Comparing the PMMA EBW to the Aluminum EBW is a challenge as not only is the casing material different, but the diameter of EBWs are different. EBWs RP-502 is most similar to RP-503, as it contains the most similar mass of explosive. Despite this, the velocities of the frag for both EBWs was observed to be very different. This indicates that further studies are needed to analyze the effect charge and casing geometry and casing material have on frag velocities.

4 | CONCLUSION

Four different detonators with different casing materials and construction were evaluated using the Gurney approximation and tested experimentally to assess how frag affects the energy distribution in the axial and radial directions. Detonators which were manufactured by metal stamping were found to have more energy loss in both the axial and radial directions compared to the detonator with its end glued to the sides (RP-503). Mathematical models predict the energy loss for cased charges to be the same regardless of the type of casing material. The stamped detonators were found to have different amounts of energy loss between them out the end, but constant along the sides.

The different material properties of the casing were found to be a contributing factor of the observed differences between the aluminum cased and PMMA cased EBWs, with PMMA having a lower difference from predicted of 21% compared to lowest error observed in Al of 28%. The percent of total explosive mass that was converted into kinetic energy was found to be 70% for the PMMA EBW and $30 \pm 3\%$ for the Al EBWs. Different materials will require different amounts of energy to fragment the casing and will affect the performance of the detonator.

Gurney equations assume that the mass of casing around an explosive is the only contributing factor to the energy distribution and considers the tensile strength of the material negligible compared to the mass of the explosive. This method is very successful for large explosives such as bombs and missiles where the energy to break the outer casing can be considered negligible. This study showed that it is not viable to evaluate the performance of small explosive charges, like detonators, because the energy needed to break the casing is not accounted for in the equations. It also poses a question of

how a high ratio of casing mass to explosive mass would affect the applicability of the Gurney equations with a large explosive mass. This study suggests that in a system, of any scale, with a high casing to explosive mass ratio, the end and side gurney equations are equally inaccurate. The level of inaccuracy is consistent among charges of the same diameter, casing material, and thickness and loss is best seen in terms of the explosive mass.

ACKNOWLEDGMENTS

Supported and funded by the Missouri University of Science and Technology Energetics Research Team, whose students, Cody Thomas and Everett Baker, helped in the execution of the experimental tests.

DATA AVAILABILITY STATEMENT

The data that support the findings of this study are available from the corresponding author upon reasonable request.

ORCID

Emily M. Johnson  <http://orcid.org/0000-0002-0670-8179>

REFERENCES

1. C. Knock, N. Davies, T. Reeves, *Propellants Explos. Pyrotech.* **2015**, *40*, 169–179.
2. G. Katselis and J. G. Anderson, *The 14th Australasian fluid mechanics conference* **2001**, *4*.
3. M. N. Plooster, Blast Effects from Cylindrical Explosive Charges: Experimental Measurements, DENVER RESEARCH INST CO, 1982.
4. C. Knock and N. Davies, *Shock Waves* **2013**, *23*, 337–343.
5. E. D. Esparza, S. Antonio, Spherical Equivalency of Cylindrical Charges in Free-Air, SOUTHWEST RESEARCH INST SAN ANTONIO TX, 1992.
6. H. Y. Grisaro, A. N. Dancygier, *International journal of impact engineering* **2015**, *86*, 1–12.
7. H. Y. Grisaro, A. N. Dancygier, *International Journal of Impact Engineering* **2016**, *94*, 13–22.
8. M. Hutchinson, *Propellants Explos. Pyrotech.* **2014**, *39.5*, 733–738.
9. C. E. Anderson, W. W. Predebon, R. R. Karpp, *Int. J. Eng. Sci.* **1985**, *23*, 1317–1330.
10. I. G. Cullis, P. Dunsmore, A. Harrison, I. Lewtas, R. Townsley, *Def. Technol.* **2014**, *10*, 198–210.
11. G. Huang, W. Li, S. Feng, *Int. J. Impact Eng.* **2015**, *76*, 20–27.
12. W. Li, G. Huang, S. Feng, *Int. J. Impact Eng.* **2015**, *80*, 107–115.
13. Q. Zhang, C.-Q. Miao, D.-C. Lin, C.-H. Bai, *Int. J. Impact Eng.* **2003**, *28*, 1129–1141.
14. J.-F. Danel, L. Kazandjian, *Propellants Explos. Pyrotech.* **2004**, *29*, 314–316.
15. P. W. Cooper in *Explosives Engineering*. New York, N. Y.: VCH, **1996**.

16. R. Gurney, The Initial Velocities of Fragments from Bombs, Shell and Grenades, Army Ballistic Research Lab Aberdeen Proving Ground Md, 1943.
17. G. E. Jones, J. E. Kennedy, L. D. Bertholf, *Am. J. Phys.* **1980**, *48*, 264–269.
18. J. E. Kennedy in *Explosive Effects and Applications*, (eds.:J. A. Zukas, W. P. Walters), Springer, New York, NY, **1998**, pp. 221–257.
19. V. Petr, E. Lozano, *Shock Waves* **2017**, *27*, 781–793.
20. M. D. Hutchinson, *Int. J. Impact Eng.* **2009**, *36*, 185–192.
21. “Phantom Camera Control (PCC) Software Tutorial Listing.” <https://phantomhighspeed-service.force.com/>.
22. “EBW Detonators.” <http://www.teledynedefenseelectronics.com/>
23. “McMaster-Carr.” <https://www.mcmaster.com/>.
24. “Energetics – Special Products.” <https://www.teledynedefenseelectronics.com/>.
25. “Global Ordnance – Global Ordnance.” <https://www.global-ordnance.com/>.
26. W. Neal, “PETN Exploding Bridgewire (EBW) Detonators: A Review,” Los Alamos National Laboratory, 2020.
27. Dobratz, B. M., LLNL Handbook of Explosives, Lawrence Livermore National Laboratory, 1981.
28. D. Frem, *Defence Technology* **2020**, *16*, 225–231.

How to cite this article: Johnson E. M., Bauer R. L. & Johnson C. E. (2023). Analyzing the effectiveness of the Gurney method for small scale fragmentation propulsion using Exploding Bridgewire detonators. *Propellants, Explosives, Pyrotechnics*, *48*, e202200246. <https://doi.org/10.1002/prop.202200246>

Graphical Abstract

The contents of this page will be used as part of the graphical abstract of html only.
It will not be published as part of main.

